**Discover** Oncology

Research

# Piezo1 regulates actin cytoskeleton remodeling to drive EMT in cervical cancer through the RhoA/ROCK1/PIP2 signaling pathway

**Juexiao Deng[1] · Yang Li[1] · Lanyue Zhang[1] · Wenxin Liao[1] · Tingting Liu[1] · Fujin Shen[1]**

Received: 10 November 2024 / Accepted: 23 April 2025
Published online: 16 May 2025


**Abstract**

**Background** Piezo1 has been identified as an oncogenic factor in various types of cancer. The objective of this study was to explore the mechanisms of Piezo1 in cervical cancer invasion and migration, with a focus on its influence on actin cytoskeleton remodeling.

**Methods** Immunohistochemistry, western blot, and dot blot assays were employed to evaluate the expression levels of Piezo1, PIP2, and F-actin in cervical cancer. Lentiviral transduction or Yoda1 treatment was used to silence or activate Piezo1. Phalloidin staining was applied to examine the actin cytoskeleton in HeLa and SiHa cells. Transwell assays were conducted to evaluate the invasive and migratory capabilities of the cells. Dot blot and ELISA assays were performed to measure the PIP2 content on the cell membrane. Western blot or qRT-PCR was used to assess the expression levels of EMT markers, RhoA, and ROCK1.

**Results** Piezo1, PIP2, and F-actin were upregulated in cervical cancer tissues, with the highest levels observed in tissues from patients with lymph node metastasis. Silencing Piezo1 downregulated the expression of F-actin and disrupted the organization of actin filaments. This cytoskeletal disruption served as an upstream event that inhibited EMT, as well as the invasion and migration of cervical cancer cells. Mechanistically, Piezo1 activated the RhoA/ROCK1 pathway, which in turn increased PIP2 levels in cervical cancer cells, leading to actin cytoskeleton remodeling in these cells.

**Conclusion** Piezo1 drives actin cytoskeleton remodeling through the RhoA/ROCK1/PIP2 signaling pathway, thereby promoting EMT, invasion, and migration in cervical cancer. Targeting Piezo1 may offer a novel therapeutic strategy, potentially improving patient outcomes.

**Keywords** Cervical cancer · Piezo1 · RhoA/ROCK1/PIP2 · Actin cytoskeleton · EMT

## 1 Introduction

Cervical cancer (CC) is the fourth leading cause of cancer-related deaths among women [1, 2], with 604,000 new cases and 342,000 deaths in 2020, resulting in a substantial global disease burden [2]. Cancer metastasis accounts for approximately 90% of cancer-related deaths [3], and in cervical cancer, 15–61% of patients experience metastatic disease within 2 years

Juexiao Deng, Yang Li and Lanyue Zhang have authors contributed equally to this work.

**Supplementary Information** The online version contains supplementary material available at https://doi.org/10.1007/s12672-025-02474-7.

✉ Fujin Shen, sfj296@163.com | [1]Department of Obstetrics and Gynecology, Renmin Hospital of Wuhan University, 239 Jiefang Road, Wuchang District, Wuhan City 430060, Hubei Province, China.

following initial treatment, significantly reducing their survival rates [4]. One of the critical mechanisms underlying cervical cancer invasion and metastasis is Epithelial–mesenchymal transition (EMT) [5]. During this process, epithelial cells lose their polarity and have an increased ability to invade and migrate, allowing them to detach from the primary tumor site and enter the bloodstream or lymphatic circulation [6, 7]. The EMT process is closely associated with actin cytoskeleton remodeling [8]. Recent studies have suggested that actin cytoskeleton reorganization may serve as an upstream event initiating the EMT process [9]. Therefore, intervening in the remodeling of the cytoskeleton may hold potential value for inhibiting cervical cancer invasion and migration.

Piezo1 is a mechanosensitive channel protein located on the plasma membrane, capable of converting extracellular mechanical signals into intracellular biochemical responses [10]. In recent years, Piezo1 has been identified as a potential therapeutic target for various cancers, due to its significant role in promoting tumor malignant progression [11–13]. Research suggests a potential interaction between Piezo1 and the actin cytoskeleton. For example, the use of cytochalasin D to disrupt actin filaments can affect the transmission of mechanical stimuli through the Piezo1 channel [14], while knockdown of Piezo1 has led to actin cytoskeleton remodeling in gastric cancer cells [15]. Currently, the functional role of Piezo1 in cervical cancer remains poorly understood. One study has reported that Piezo1 promotes the invasion and migration of cervical cancer cells by facilitating the release of ATP [16]. However, the role of Piezo1 in actin cytoskeleton remodeling and its underlying mechanisms in cervical cancer have yet to be elucidated.

Phosphatidylinositol (4,5)-bisphosphate (PIP2) is the most abundant phosphoinositide in the cell membrane and serves as a critical component of lipid rafts. PIP2 plays a regulatory role in various essential biological processes, including modulating the activity of cytoskeletal-binding proteins [17–19], influencing transporter functions and participating in cancer pathogenesis [20, 21]. Studies have demonstrated that PIP2 levels are elevated in cells with high proliferation and motility [22],however, its expression levels in cervical cancer have not yet been reported. Recent research has revealed that PIP2 forms a negatively charged annular structure around Piezo1, interacting strongly with specific Piezo1 residues. Interestingly, no other lipids were found to form similar clustered or ring-like structures around Piezo1 [23]. Whether Piezo1 regulates PIP2 remains unclear. The RhoA/ROCK1 pathway, recognized as mechanosensitive, has been shown to inhibit PIP2-induced cytoskeletal remodeling in mouse cardiomyocytes when selectively suppressed [24], suggesting that PIP2 may act as a key downstream effector of the RhoA/ROCK1 pathway.

In this study, we demonstrated that the overexpression of Piezo1 in cervical cancer cells activates the RhoA/ROCK1 signaling pathway, resulting in elevated PIP2 levels. This activation subsequently drives the remodeling of the actin cytoskeleton, thereby promoting EMT. Consequently, the migratory and invasive capabilities of the cancer cells were significantly enhanced. These findings suggest that targeting Piezo1 may provide a promising therapeutic strategy for inhibiting the invasion and migration of cervical cancer cells.

## 2 Methods

### 2.1 Cell culture

The cervical cancer cell lines HeLa, SiHa, C33A, and the normal cervical epithelial cell line HUCEC were cultured in high-glucose DMEM (HyClone, USA, Cat. No. SH30022.01) supplemented with 10% fetal bovine serum (Yeasen, China, Cat. No. 40130ES76) and 1% penicillin–streptomycin (Biosharp, China, Cat. No. BL505A). Cells were incubated at 37 °C with 5% $CO_2$.

### 2.2 Reagents and inhibitors

Rhosin hydrochloride (20 μM, MCE, China, Cat. No. HY-12646) and Y-27632 (10 μM, MCE, China, Cat. No. HY-10071) were used to inhibit RhoA and ROCK1 activation, respectively, for 24 h. PIP2 reagent (500 ng/L, Echelon Biosciences, China, Cat. No. P-4508) was added to the medium for 12 h. Neomycin (500 μM, MCE, China, Cat. No. HY-B0470), which has a high affinity for PIP2, was used to treat cervical cancer cell lines for 24 h to inhibit the function of PIP2 on the cell membrane [25]. The actin polymerization inducer Jasplakinolide (0.1 μM, Absin, China, Cat. No. 102396-24-7), the actin depolymerizing agent Latrunculin A (0.2 μM, MCE, China, Cat. No. HY-16929), and the Piezo1 activator Yoda1 (5 μM, MCE, China, Cat. No. HY-18723) were co-cultured with cells for 24 h.

### 2.3 Lentiviral infection

HeLa and SiHa cells were seeded in 6-well plates at a density of $5 \times 10^5$ cells per well. After cell adhesion, an appropriate volume of lentivirus and HitransG A solution was added to initiate infection. Following a 16 h incubation and medium change, puromycin selection (2 μg/mL for HeLa and 2.5 μg/mL for SiHa) was applied for 48 h to eliminate uninfected cells. Infection efficiency was evaluated by fluorescence microscopy. Piezo1 expression levels were then quantified using Western blot and qRT-PCR analyses.

### 2.4 Transwell assay

For assessing invasion, Matrigel (Corning, USA, Cat. No.354234), diluted 1:8 in serum-free DMEM, was used to coat the upper chamber overnight. Cells ($1 \times 10^5$) in serum-free DMEM were added to the upper chamber, while the lower chamber contained 10% FBS DMEM as a chemoattractant. After 48 h, the cells were fixed, stained with crystal violet, and non-invading cells were removed. For migration assays, the same steps were followed, but without the Matrigel coating, with $5 \times 10^4$ cells seeded in the upper chamber. Cell counts were performed using ImageJ.

### 2.5 Phalloidin staining

Cells were seeded on sterile glass coverslips and incubated overnight for adhesion. After fixation with 4% paraformaldehyde for 15 min, rhodamine-labeled phalloidin (ABclonal, China, Cat. No. RM02835) was diluted to 1:80 and applied for 45 min to stain F-actin. Nuclei were counterstained with DAPI, and images were captured under a fluorescence microscope.

### 2.6 Western blot

Cells were lysed with RIPA buffer (Beyotime, China, Cat. No. P0013B) containing 1% protease inhibitor and 1% phenylmethylsulfonyl fluoride (MCE, China, Cat. No. HY-B0496). Protein concentrations were determined using the BCA method. SDS-PAGE was used for protein separation, and proteins were transferred to a PVDF membrane (Millipore, USA, Cat. No. IPVH00010). The membrane was blocked with 5% non-fat milk for 2 h and then incubated overnight at 4 °C with primary antibodies: Piezo1 (Proteintech, China, Cat. No. 15939-1-AP), E-cadherin (Proteintech, China, Cat. No. 20874-1-AP), N-cadherin (Proteintech, China, Cat. No. 66219-1-lg), Vimentin (Proteintech, China, Cat. No. 60330-1-lg), and GAPDH (Proteintech, China, Cat. No. 10494-1-AP). The following day, the membrane was incubated with an HRP-conjugated secondary antibody for 1 h. Protein bands were visualized using a gel imaging system and Clarity Western ECL substrate (Biosharp, China, Cat. No. BL523B).

### 2.7 Quantitative real-time PCR (qRT-PCR)

Total RNA was extracted from cervical cancer cells using Trizol reagent, and the RNA concentration was quantified. Reverse transcription was performed according to the manufacturer's protocol (Yeasen, China, Cat. No. 11141ES60). Primers for Piezo1, RhoA, ROCK1, and GAPDH were synthesized by Sangon Biotech (China). qRT-PCR was conducted using SYBR Green reagent, and all procedures were meticulously followed according to the kit protocols (Yeasen, China, Cat. No. 11185ES08).

### 2.8 Dot blot

Cells were lysed using RIPA lysis buffer containing protease inhibitor, phosphatase inhibitor (Servicebio, China, Cat. No. G2007-1ML), and phenylmethylsulfonyl fluoride, followed by sonication for 5 min. Protein concentration was determined using the BCA assay. The lysates were then spotted onto a nitrocellulose membrane. After blocking with 5% non-fat milk for 2 h, the membrane was incubated overnight at 4 °C with primary antibodies: PIP2 (Santa Cruz, USA, Cat. No. sc-53412) and GAPDH (Proteintech, China, Cat. No. 10494-1-AP). The following day, HRP-conjugated secondary antibodies were applied for 1 h. Protein expression levels of PIP2 and GAPDH were detected using a gel imaging system with Clarity Western ECL substrate (Biosharp, China, Cat. No. BL523B).

**Fig. 1** Upregulation of Piezo1, PIP2, and F-actin in cervical cancer. CC, cervical cancer. **A**, **B**, **C**, **D**, **E**, **F** Immunohistochemical analysis of Piezo1, PIP2, and F-actin expression levels in cervical cancer tissues with lymph node metastasis (n = 5), without lymph node metastasis (n = 18), and in normal cervical tissues (n = 11), with quantification provided. Scale bar: 50 μm. **G**, **I** Western blot analysis showing Piezo1 protein expression levels in the normal cervical epithelial cell line HUCEC and cervical cancer cell lines HeLa, SiHa, and C33A, with quantification. **H**, **J** Dot blot analysis of PIP2 expression levels in the normal cervical epithelial cell line HUCEC and cervical cancer cell lines HeLa, SiHa, and C33A, along with quantification. *$P < 0.05$; **$P < 0.01$; ***$P < 0.001$; ****$P < 0.0001$

### 2.9 Enzyme-linked immunosorbent assay (ELISA)

For the PIP2 ELISA assay, cell lysates were prepared as described for the Dot blot. Standards were prepared according to the manufacturer's instructions for the PIP2 ELISA kit (MEIMIAN, China, Cat. No. MM-12437H1). Fifty microliters of five-fold diluted lysate were added to each well, followed by 100 μL of HRP-conjugated secondary antibody. The plate was incubated at 37 °C for 1 h. After five washes, 50 μL of Substrate A and B were added, and incubation continued in the dark at 37 °C for 15 min. The reaction was stopped by adding 50 μL stop buffer, and optical density (OD) was measured at 450 nm. Sample concentrations were determined from the standard curve.

### 2.10 Cases and samples

In this study, 34 patients who received surgical treatment or biopsy at Renmin Hospital of Wuhan University between June 2023 and May 2024 were analyzed. The cohort consisted of 18 patients with non-metastatic cervical cancer, 5 patients with lymph node metastasis, and 11 patients who underwent hysterectomy for benign uterine conditions. Ethical approval was obtained from the Ethics Committee of Renmin Hospital of Wuhan University (Ethics number: WDRY2023-K092), and informed consent was obtained from all participants. The clinical pathological characteristics of the patients have been summarized in Supplementary Table 1, with personal privacy information removed.

### 2.11 Immunohistochemical staining

Fresh cervical tissue samples were fixed, paraffin-embedded, and sectioned, followed by deparaffinization and rehydration. Antigen retrieval was performed by heating the sections in citrate buffer. Next, the sections were incubated with 3% hydrogen peroxide for 10 min and blocked with 10% goat serum for 1 h. Overnight incubation with primary antibodies against Piezo1 (Proteintech, China, Cat. No. 15939-1-AP), F-actin (Abcam, UK, Cat. No. ab130935), and PIP2 (Santa Cruz, USA, Cat. No. sc-53412) was then performed. The following day, the sections were incubated with the corresponding HRP-conjugated secondary antibodies for 30 min, followed by DAB staining. Nuclei were counterstained with hematoxylin. The positively stained areas were quantitatively analyzed using ImageJ software.

### 2.12 Statistical analysis

The experimental data were analyzed using GraphPad Prism 9. Continuous variables were presented as the mean ± standard deviation (SD). One-way analysis of variance (ANOVA) was used to compare multiple independent sample groups, while t tests were employed for comparisons between two groups. $P < 0.05$ was considered statistically significant.

## 3 Results

### 3.1 Upregulation of Piezo1, PIP2, and F-actin in cervical cancer

To assess the roles of Piezo1, PIP2, and F-actin in cervical cancer, their expression levels were evaluated in tissue samples and cell lines. Immunohistochemistry was first employed to examine the expression of Piezo1, PIP2, and F-actin in normal cervical tissues, primary cervical cancer tissues with lymph node metastasis, and cervical cancer tissues without lymph node metastasis. All three markers showed low expression in normal cervical tissues but exhibited significantly higher expression in cancer tissues. Notably, the expression of these markers was highest in the primary cervical cancer tissues with lymph node metastasis (Fig. 1A, B, C, D, E, F). We also used western blot to further assess the expression levels of Piezo1 in the three types of cervical tissues mentioned above (Figure S1A, B), and the results were consistent with

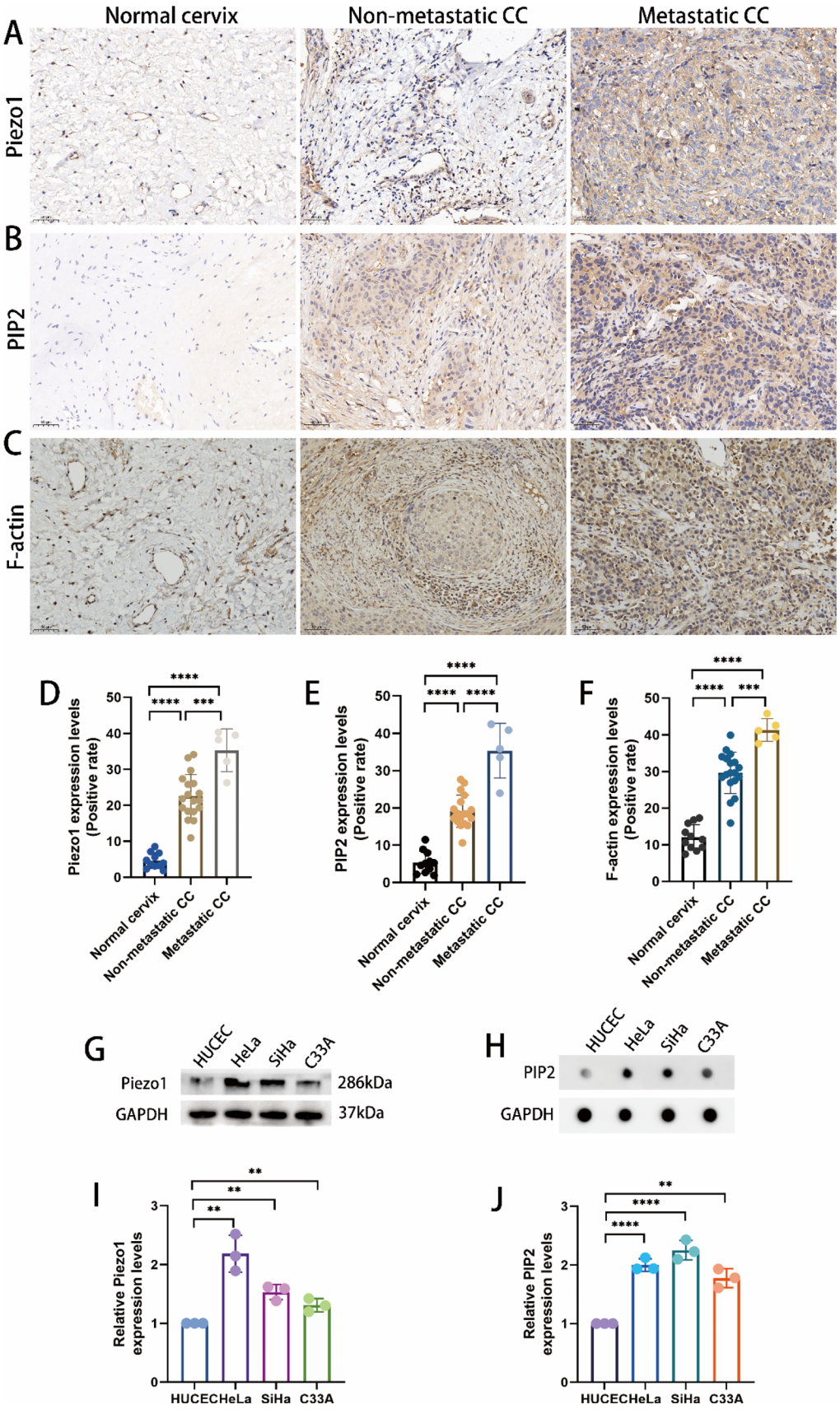
Normal cervix
Non-metastatic CC
Metastatic CC
A
Piezo1
B
PIP2
C
F-actin
D
Piezo1 expression levels (Positive rate)
E
PIP2 expression levels (Positive rate)
F
F-actin expression levels (Positive rate)
Normal cervix
Non-metastatic CC
Metastatic CC
G
HUCEC
HeLa
SiHa
C33A
Piezo1
286kDa
GAPDH
37kDa
H
PIP2
GAPDH
I
Relative Piezo1 expression levels
J
Relative PIP2 expression levels

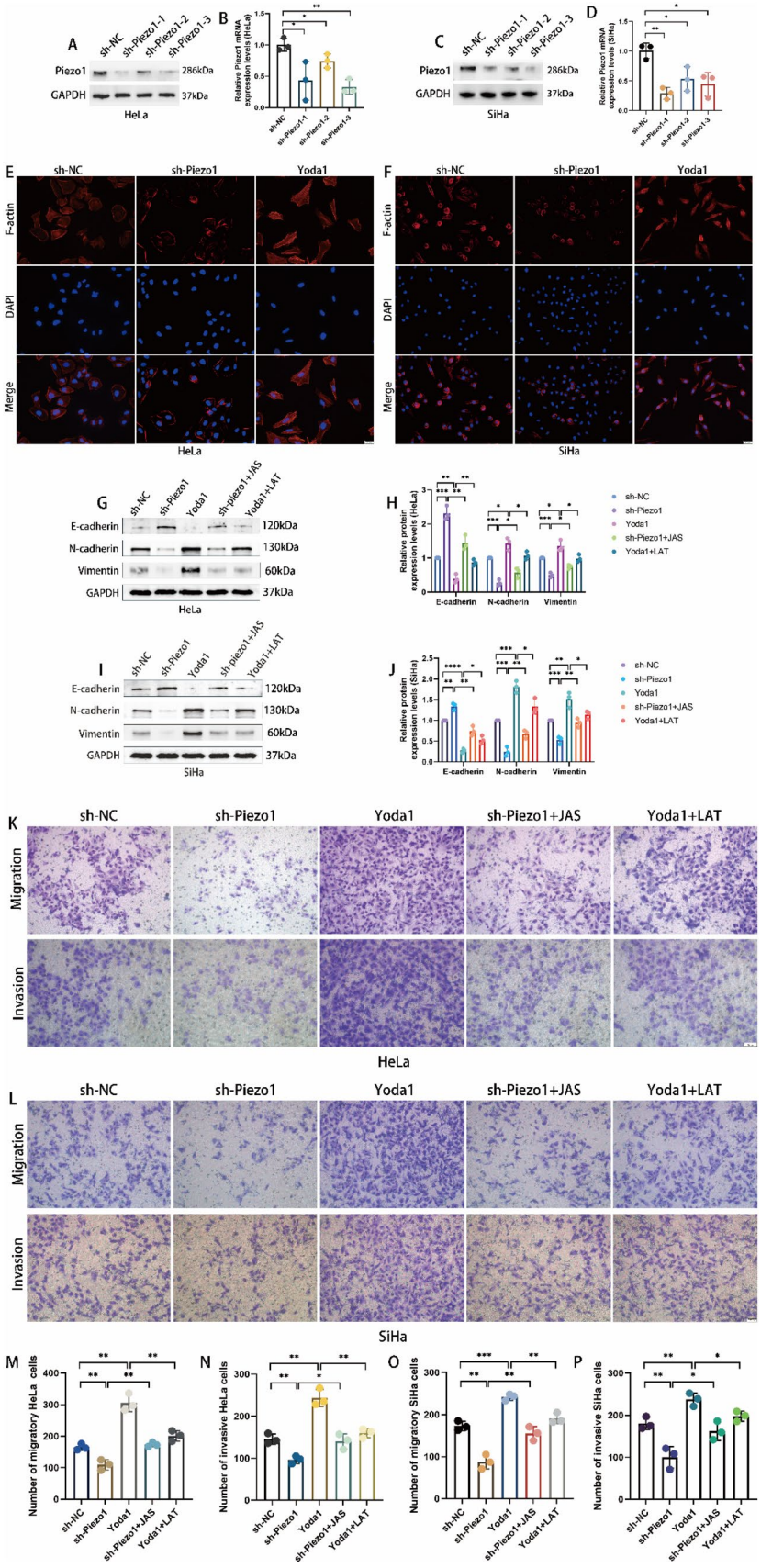
A
sh-NC
sh-Piezo1-1
sh-Piezo1-2
sh-Piezo1-3
Piezo1
286kDa
GAPDH
37kDa
HeLa
B
Relative Piezo1 mRNA expression levels (HeLa)
C
SiHa
D
Relative Piezo1 mRNA expression levels (SiHa)
E
F
sh-Piezo1
Yoda1
F-actin
DAPI
Merge
G
sh-Piezo1+JAS
Yoda1+LAT
E-cadherin
120kDa
N-cadherin
130kDa
Vimentin
60kDa
H
Relative protein expression levels (HeLa)
I
J
Relative protein expression levels (SiHa)
K
Migration
Invasion
L
M
Number of migratory HeLa cells
N
Number of invasive HeLa cells
O
Number of migratory SiHa cells
P
Number of invasive SiHa cells

◂**Fig. 2** Piezo1 drives cervical cancer EMT by regulating actin cytoskeleton remodeling. The sh-NC group consisted of cells transfected with a negative control virus; the sh-Piezo1 group included cells transfected with Piezo1 knockdown virus; the Yoda1 group contained sh-NC cells treated with Yoda1 to activate Piezo1; the sh-Piezo1 + Jasplakinolide (JAS) group included sh-Piezo1 cells treated with the actin polymerization agent Jasplakinolide (JAS) to induce actin polymerization in Piezo1 knockdown cells; and the Yoda1 + Latrunculin A (LAT) group consisted of sh-NC cells treated with both Yoda1 and the actin depolymerizing agent Latrunculin A (LAT) to induce actin depolymerization in Yoda1-activated cells. **A**, **B**, **C**, **D** HeLa and SiHa cells were transfected with Piezo1-targeting lentiviruses (including negative control sh-NC and interference sequences sh-Piezo1-1, sh-Piezo1-2, and sh-Piezo1-3). Western blotting and qRT-PCR were performed to assess the efficiency of Piezo1 knockdown. **E**, **F** Phalloidin staining was used to observe the F-actin cytoskeleton in HeLa and SiHa cells from the control group, sh-Piezo1 group, and Yoda1-treated group. Scale bar: 20 μm. **G**, **H**, **I**, **J** Western blotting analysis of EMT markers E-cadherin, N-cadherin, and Vimentin expression in HeLa and SiHa cells from the sh-NC group, sh-Piezo1 group, Yoda1 group, sh-Piezo1 + Jasplakinolide (JAS) group, and Yoda1 + Latrunculin A (LAT) group, with quantification. **K**, **L**, **M**, **N**, **O**, **P** Representative images and quantification of transwell assays evaluating migration and invasion abilities of HeLa and SiHa cells from the sh-NC group, sh-Piezo1 group, Yoda1 group, sh-Piezo1 + Jasplakinolide (JAS) group, and Yoda1 + Latrunculin A (LAT) group. Scale bar: 50 μm. $^{*}P < 0.05$; $^{**}P < 0.01$; $^{***}P < 0.001$; $^{****}P < 0.0001$

the aforementioned findings. Subsequently, western blot and dot blot analyses were used to assess the expression of Piezo1 and PIP2 in the normal cervical epithelial cell line (HUCEC) and cervical cancer cell lines (HeLa, SiHa, and C33A). The results revealed higher expression levels of both markers in the cervical cancer cell lines (Fig. 1G, H, I, J). Due to the depolymerization of F-actin during cell lysis, western blotting was not performed to evaluate its expression in the cell lines. These findings suggest that Piezo1, PIP2, and F-actin may play critical roles in the metastatic process of cervical cancer. Additionally, all 34 patients underwent human papillomavirus (HPV) genotyping before surgery (the results are provided in Supplementary Table 1). Among the cervical cancer patients, 7 were HPV-positive and 16 were HPV-negative, while none of the patients with benign conditions tested positive for HPV infection. Based on HPV infection status, the 23 cervical cancer patients were divided into two groups: HPV-positive and HPV-negative. We compared the Piezo1 protein levels between the two groups using corresponding immunohistochemical results. Our analysis revealed no significant association between Piezo1 expression and HPV infection status in our clinical samples, with no statistically significant differences observed (Fig. S2).

### 3.2 Piezo1 drives cervical cancer EMT by regulating actin cytoskeleton remodeling

In this section, we first investigated the impact of Piezo1 on the actin cytoskeleton. Stable Piezo1 knockdown cell lines were generated by transducing HeLa and SiHa cells with lentiviral vectors. Western blotting and qRT-PCR were performed to verify transfection efficiency (Fig. 2A, B, C, D), with sh-Piezo1-3 selected for further experiments (hereafter referred to as sh-Piezo1). Phalloidin, a phallotoxin that specifically binds to filamentous actin (F-actin), was used to visualize F-actin levels. Our results demonstrated that, compared to the control group, F-actin levels were reduced in the sh-Piezo1 group, with the actin structure appearing loose and irregular. Conversely, upon treatment with the Piezo1-specific agonist Yoda1, the cytoplasmic F-actin levels were significantly increased, with a denser and more organized arrangement (Fig. 2E, F).

We subsequently examined the impact of Piezo1 on EMT in cervical cancer cells. When Piezo1 was silenced, an increase in E-cadherin protein levels was observed in both HeLa and SiHa cells, along with a decrease in N-cadherin and Vimentin levels. Conversely, activation of Piezo1 using the agonist Yoda1 produced the opposite effect, with E-cadherin downregulated and N-cadherin and Vimentin levels elevated (Fig. 2G, H, I, J.

Recent studies have reported that the actin cytoskeleton can serve as an upstream driver of the EMT process in murine hepatocellular carcinoma cells [9]. We were intrigued to investigate whether a similar regulatory pathway exists in cervical cancer. Jasplakinolide, a natural macrocyclic peptide, promotes the polymerization of actin monomers into filamentous actin (F-actin) [26], whereas Latrunculin A, an actin filament depolymerizing agent, facilitates the disassembly of F-actin into monomeric actin [27]. These agents allowed us to modulate the polymerization state of the actin cytoskeleton in our experiments. In subsequent experiments, we co-cultured Jasplakinolide with Piezo1-silenced cells. Interestingly, this co-treatment reversed the upregulation of E-cadherin, while N-cadherin and Vimentin were upregulated. Conversely, when Yoda1 and Latrunculin A were co-cultured in HeLa and SiHa cells, E-cadherin expression, which was initially downregulated by Yoda1, was restored, and N-cadherin and Vimentin levels decreased (Fig. 2G, H, I, J). These results suggest a regulatory role of actin cytoskeleton remodeling in modulating EMT in cervical cancer cells. In addition, we assessed the invasive and migratory abilities of cells in the five experimental groups using a transwell assay. The results indicated that, compared to the sh-NC group, silencing Piezo1 expression (sh-Piezo1) or activating Piezo1 (Yoda1) inhibited and promoted the invasion and migration abilities of cervical cancer cells, respectively. Notably, when sh-Piezo1 cells were treated with Jasplakinolide, the inhibitory effects of Piezo1 knockdown on invasion and migration were partially reversed. However, when Yoda1-treated cells were treated with Latrunculin A, the promoting effects of Piezo1 activation

on invasion and migration were significantly diminished (Fig. 2K, L, M, N, O, P). These findings provide evidence that Piezo1 drives EMT and invasion and migration in cervical cancer through the regulation of actin cytoskeleton remodeling.

### 3.3 PIP2 regulates actin cytoskeletal remodeling

Our study confirmed the upregulation of PIP2 in human cervical cancer tissues. As an important phospholipid in the cell membrane, PIP2 plays a regulatory role in various cytoskeletal-binding proteins. To investigate whether changes in PIP2 levels can affect the actin cytoskeleton in cervical cancer cells, we treated HeLa and SiHa cells with the PIP2 inhibitor neomycin. We observed a decrease in F-actin levels and a more dispersed structure. In contrast, cells treated with PIP2 exhibited a significant increase in F-actin levels (Fig. 3A, B). Furthermore, we conducted transwell assays to assess the impact of PIP2 levels on the invasion and migration characteristics of cervical cancer cells. After neomycin treatment, the invasion and migration abilities of HeLa and SiHa cells were reduced, while PIP2 treatment enhanced the invasion and migration capacities of the cervical cancer cells (Fig. 3C, D, E, F, G, H).

### 3.4 Piezo1 remodels the actin cytoskeleton by upregulating PIP2 levels

Dot blot and ELISA assays were used to investigate the effect of Piezo1 on PIP2 levels. When Piezo1 was silenced in HeLa and SiHa cells, PIP2 levels were found to be downregulated. In contrast, treatment with the Piezo1-specific agonist Yoda1 led to an increase in PIP2 content (Fig. 4A, B, C, D, E, F). Furthermore, we aimed to determine whether Piezo1 regulates actin cytoskeleton remodeling through PIP2. Phalloidin staining revealed an increase in F-actin levels and more orderly arrangement in the Yoda1-treated group compared to the control group. However, when PIP2 inhibitor neomycin was added to the Yoda1-treated group, the effects induced by Yoda1 were abolished (Fig. 4G, H). These results suggest that Piezo1 may regulate the actin cytoskeleton via PIP2. Additionally, we observed changes in the invasion and migration capabilities of HeLa and SiHa cells. Neomycin was found to abolish the pro-invasive and pro-migratory effects of Yoda1 on these cells (Fig. 4I, J, K, L, M, N).

### 3.5 Piezo1 increases PIP2 levels in cervical cancer cells by activating the RhoA/Rock1 signaling pathway

In this section, we sought to further investigate the mechanism by which Piezo1 influences PIP2. Initially, the effect of Piezo1 on the RhoA/Rock1 pathway was studied in HeLa and SiHa cells. The results demonstrated that, compared to the sh-NC group, the expression levels of RhoA and Rock1 proteins were reduced in the sh-Piezo1 group, while their expression was upregulated in the Yoda1 group (Fig. 5A). Similar findings were observed through qRT-PCR experiments (Fig. 5B, C, D, E). Next, we utilized dot blot and ELISA assays to investigate the impact of RhoA/Rock1 on PIP2. Our results showed that the effects of Yoda1 on PIP2 were abolished by the RhoA inhibitor Rhosin hydrochloride or the ROCK1 inhibitor Y-27632 (Fig. 5F, G, H, I, J, K). Overall, we propose that Piezo1 regulates the actin cytoskeleton in cervical cancer cells by enhancing PIP2 levels through the activation of the RhoA/ROCK1 pathway.

## 4 Discussion

Cervical cancer remains a major threat to women's health worldwide [28]. While current treatment strategies are effective for early-stage cervical cancer, the clinical outcomes for patients with metastatic or lymph node-positive cervical cancer remain poor [29]. The precise molecular mechanisms underlying cervical cancer invasion and metastasis are not yet fully understood. Piezo1, a mechanically sensitive large cation channel protein, has been found to be aberrantly overexpressed in tumors of the digestive, reproductive, and urinary systems, where it mediates malignant behaviors such as proliferation, invasion, and metastasis [11–13]. In this study, Piezo1 was observed to be significantly overexpressed in cervical cancer. Notably, primary cervical cancer tissues from patients with lymph node metastases exhibited even higher levels of Piezo1 expression, suggesting a potential role for Piezo1 in promoting cervical cancer metastasis. Metastasis is a complex process requiring cancer cells to overcome multiple barriers. After degrading the extracellular matrix and basement membrane [30], cancer cells enter the vasculature or lymphatic system, where they are exposed to elevated fluid shear stress, which can lead to cell damage or even death [31]. Studies have shown that fluid shear stress induces membrane deformation, activating membrane-bound Piezo1,this activation translates mechanical forces into biochemical signals, enhancing the ability to withstand physical stress of cells [32, 33], this observation may partly

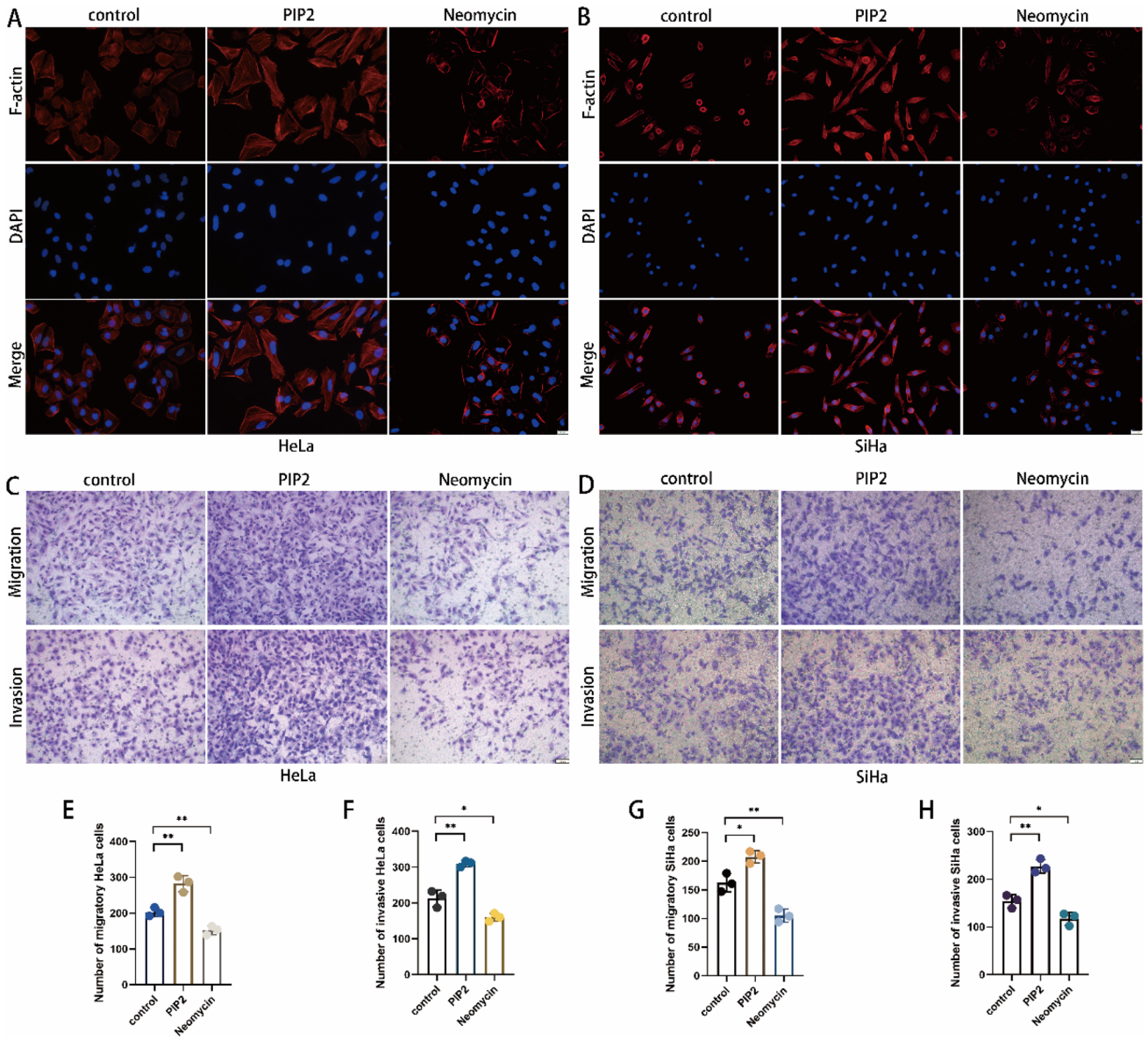


**Fig. 3** PIP2 regulates actin cytoskeletal remodeling. **A**, **B** Phalloidin staining was used to observe the actin cytoskeleton in HeLa and SiHa cells from the control group, PIP2 group, and Neomycin group. Scale bar:20 μm. **C**, **D**, **E**, **F**, **G**, **H** Representative images and quantitative analysis from transwell assays were used to assess the migration and invasion abilities of HeLa and SiHa cells in the control group, PIP2 group, and Neomycin group. Scale bar:50 μm. *$P < 0.05$; **$P < 0.01$; ***$P < 0.001$; ****$P < 0.0001$

explain the higher expression levels of Piezo1 in patients with lymph node metastases. Given that HPV infection remains the primary risk factor for cervical cancer [34], we divided the 23 cervical cancer samples we collected into HPV-positive and HPV-negative groups. The results showed no significant differences in Piezo1 protein expression levels between the two groups. In other words, no correlation between Piezo1 expression and HPV infection status was observed in our limited clinical samples. However, in our cell experiments, HeLa cells (HPV-18 positive) exhibited higher Piezo1 expression compared to SiHa cells (HPV-16 positive) and C33A cells (HPV-negative), which we speculate may be due to the inherent characteristics of the cells. Nonetheless, the association between Piezo1 expression levels and HPV infection status still requires further validation through larger sample sizes.

The cytoskeleton comprises microtubules, microfilaments, and intermediate filaments [35]. Microfilaments, also known as the actin cytoskeleton, are composed of actin monomers (G-actin) and serve as critical components for maintaining cell shape and enabling movement. Through dynamic remodeling, they play a pivotal role in driving tumor cell invasion and migration [36, 37]. Previous studies have suggested intricate connections between Piezo1 and the actin cytoskeleton.

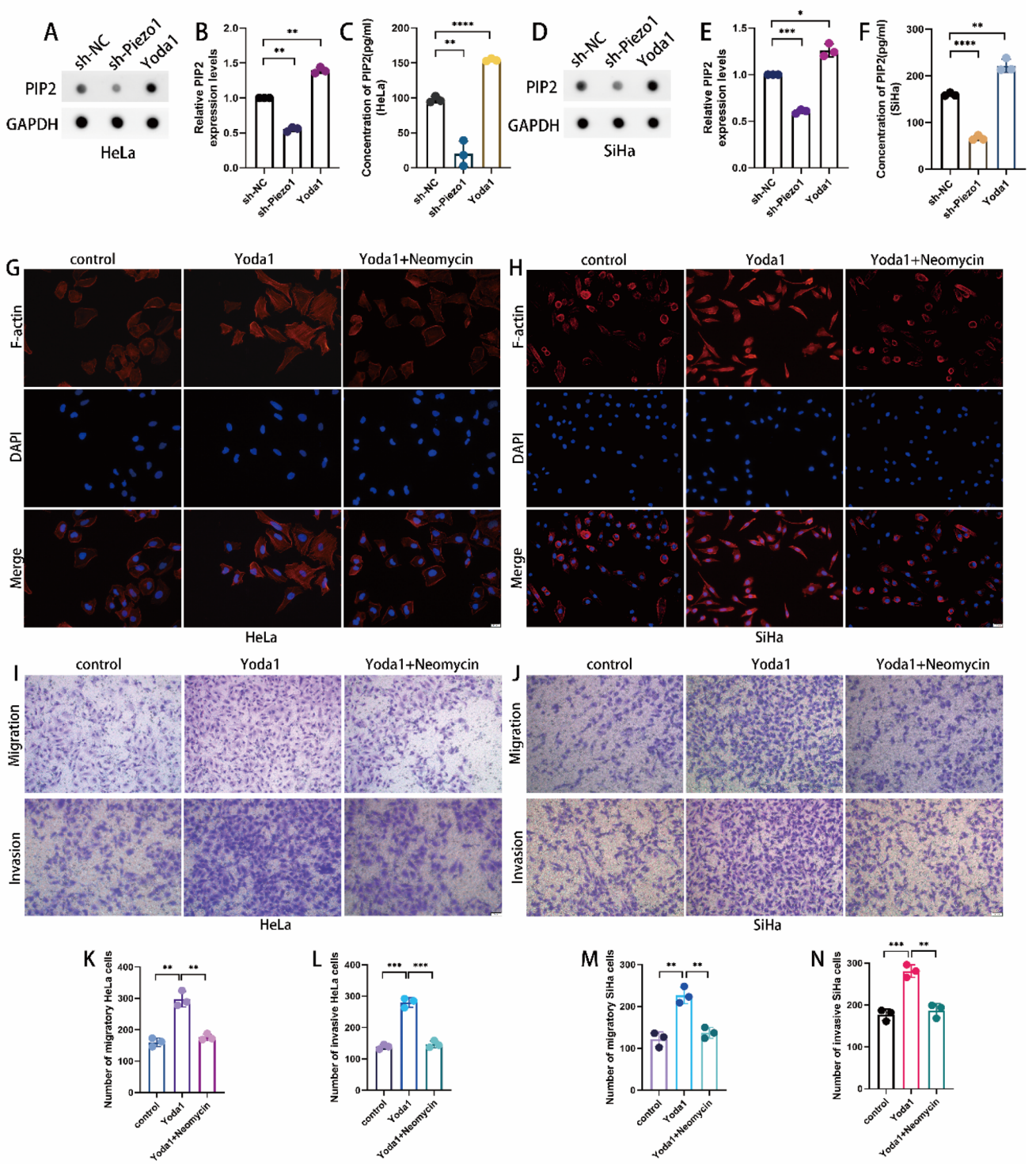


**Fig. 4** Piezo1 remodels the actin cytoskeleton by upregulating PIP2 levels. **A**, **B** Dot blot analysis shows the expression of PIP2 in HeLa cells from the sh-NC, sh-Piezo1, and Yoda1 groups, along with their respective quantification. **C** ELISA assay was used to analyze the expression of PIP2 in HeLa cells from the sh-NC, sh-Piezo1, and Yoda1 groups. **D**, **E** Dot blot analysis shows the expression of PIP2 in SiHa cells from the sh-NC, sh-Piezo1, and Yoda1 groups, along with their respective quantification. **F** ELISA assay was used to analyze the expression of PIP2 in SiHa cells from the sh-NC, sh-Piezo1, and Yoda1 groups. **G**, **H** Phalloidin staining was performed to observe the actin cytoskeleton in HeLa and SiHa cells from the control, Yoda1, and Yoda1 + Neomycin groups. Scale bar:20 μm. **I**, **J**, **K**, **L**, **M**, **N** Transwell assays were performed to evaluate the migration and invasion abilities of HeLa and SiHa cells from the control, Yoda1, and Yoda1 + Neomycin groups, along with representative images and their quantification. Scale bar:50 μm. $^{*}P < 0.05$; $^{**}P < 0.01$; $^{***}P < 0.001$; $^{****}P < 0.0001$

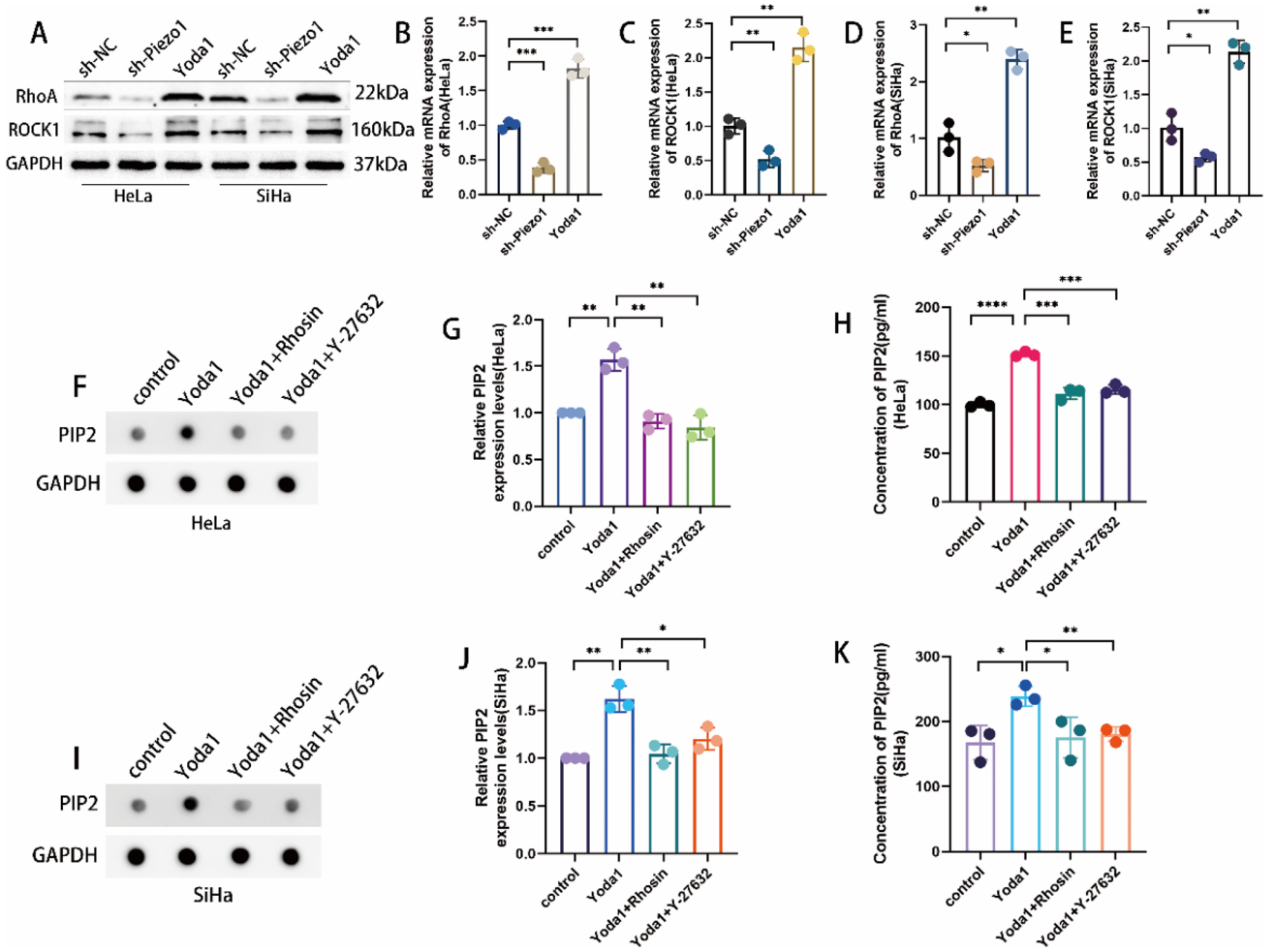


**Fig. 5** Piezo1 increases PIP2 levels in CC cells by activating the RhoA/Rock1 signaling pathway. **A** Western blot analysis was performed to assess the expression levels of RhoA and ROCK1 proteins in HeLa and SiHa cells from the sh-NC, sh-Piezo1, and Yoda1 groups. **B**, **C**, **D**, **E** qRT-PCR analysis was used to determine the mRNA expression levels of RhoA and ROCK1 in HeLa and SiHa cells from the sh-NC, sh-Piezo1, and Yoda1 groups. **F**, **G** Dot blot analysis revealed the PIP2 expression levels and their quantification in HeLa cells from the control, Yoda1, Yoda1 + Rhosin, and Yoda1 + Y-27632 groups. **H** ELISA assay was performed to quantify PIP2 expression in HeLa cells from the aforementioned groups. **I**, **J** Dot blot analysis displayed the PIP2 expression levels and their quantification in SiHa cells from the control, Yoda1, Yoda1 + Rhosin, and Yoda1 + Y-27632 groups. **K** ELISA assay was conducted to assess PIP2 expression in SiHa cells from these groups. $^{*}P < 0.05$; $^{**}P < 0.01$; $^{***}P < 0.001$; $^{****}P < 0.0001$

For instance, upon Yoda1 stimulation, bone marrow-derived macrophages (BMDMs) exhibit F-actin accumulation, which is essential for their phagocytic function [38]. A similar effect has been observed in optic nerve head astrocytes, where Yoda1 treatment induces actin cytoskeleton remodeling and a significant increase in F-actin levels [39]. Our study further confirmed the regulatory role of Piezo1 in the organization of the actin cytoskeleton. Specifically, downregulation of Piezo1 disrupted actin filament structures, whereas activation of Piezo1 by its agonist Yoda1 significantly enhanced the organized arrangement of cytoplasmic actin filaments. Epithelial-mesenchymal transition (EMT) is a crucial biological process through which tumor cells acquire migratory and invasive capabilities. During EMT, the actin cytoskeleton undergoes significant remodeling, supporting changes in cell morphology. This transition enables cells to shift from a polarized, tightly connected epithelial phenotype to a mesenchymal phenotype characterized by enhanced motility and independent migration [8], which is marked by the downregulation of the epithelial marker E-cadherin and upregulation of mesenchymal markers N-cadherin and Vimentin. Our findings indicate that Piezo1 serves as a positive regulator of EMT, consistent with previous research [40]. Downregulation of Piezo1 was observed to significantly suppress EMT, highlighting its role in promoting this critical process. To further investigate whether Piezo1 influenced EMT through the regulation of actin cytoskeleton remodeling, we treated cells with Jasplakinolide and Latrunculin A to modulate actin

polymerization. Our findings aligned with those of Peng et al. [9], indicating that actin cytoskeleton reorganization may have served as an upstream event initiating the EMT process.

PIP2 is a multifunctional phospholipid and a major component of lipid rafts. It serves as a critical molecule in signal transduction pathways at the cell membrane and plays a key role in regulating actin cytoskeleton remodeling, thereby influencing cell migration [41]. This regulatory function of PIP2 is primarily mediated through its ability to modulate the activity of various actin-binding proteins, accumulating evidence suggests that PIP2 often inactivates actin-binding proteins that inhibit actin polymerization, while activating those that promote it [18, 42]. Our study, for the first time, demonstrated that PIP2 is highly expressed in cervical cancer tissues compared to normal cervical tissues. In cervical cancer cell lines HeLa and SiHa, the addition of PIP2 significantly increased F-actin levels, leading to a denser and more organized arrangement of actin filaments. Conversely, depletion of membrane PIP2 resulted in a disrupted and disorganized actin filament structure. Thus, we report that elevated PIP2 levels in cervical cancer contribute to the remodeling of the actin cytoskeleton. As mentioned earlier, Piezo1 may have a strong interaction with PIP2 [23]. Previous studies have indicated that the activity of the Piezo1 channel requires the presence of PIP2, as the depletion of PIP2 reduces Piezo1 channel activity [43]. However, it remains unclear whether Piezo1 regulates PIP2. In our study, we found that PIP2 levels decrease upon Piezo1 knockdown, whereas the use of the agonist Yoda1 significantly increases PIP2 levels in cervical cancer cells. More importantly, the regulatory effect of Piezo1 on the actin cytoskeleton is mediated through PIP2, as the PIP2 inhibitor Neomycin can counteract the role of Yoda1 in cytoskeletal remodeling.

Rho-associated coiled-coil kinase (ROCK)are established effectors of the small GTPase RhoA [44]. The RhoA/ROCK signaling pathway plays a pivotal role in regulating actin cytoskeleton dynamics, a function well-documented in both tumor and non-tumor contexts [45, 46]. In a study on gastric cancer, Piezo1 was found to modulate the activity of Rho GTPase family members, maintaining the cell morphology associated with the motility of gastric cancer (GC) cells. Silencing Piezo1 led to a significant downregulation of RhoA expression [15]. Similarly, our findings demonstrated that silencing Piezo1 reduced the expression levels of both RhoA and ROCK1. PIP2, identified as a critical downstream molecule of the RhoA/ROCK pathway in some studies, plays a key role in actin cytoskeleton remodeling. For instance, Huang et al. reported that activation of the RhoA/ROCK1 pathway promoted PIP2 synthesis in hepatocellular carcinoma cells [25]. Consistent with these findings, our research revealed that Piezo1 activates the RhoA/ROCK1 signaling pathway, thereby increasing PIP2 levels in cervical cancer cells. Moreover, inhibitors targeting this pathway, such as Rhosin hydrochloride and Y-27632, effectively suppressed Yoda1-induced PIP2 level changes in cervical cancer cells. Although the Piezo1/RhoA/ROCK1/PIP2 signaling pathway has been confirmed in our study, it is possible that other signaling pathways may also mediate the pro-tumorigenic effects of Piezo1, such as promoting invasion, migration, and epithelial-mesenchymal transition (EMT). For instance, Piezo1 has been shown to promote EMT in hepatocellular carcinoma by activating the TGF-β signaling pathway [40], and to enhance invasion and migration in ovarian cancer via the Hippo/YAP pathway [47]. Our research demonstrates that Piezo1 induces actin cytoskeleton remodeling through the RhoA/ROCK1/PIP2 pathway, which in turn influences EMT and cellular invasion and migration. Future studies could further investigate other potential mechanisms by which Piezo1 affects actin cytoskeleton dynamics.

Given that Piezo1 plays a key role in several disease-related biological pathways, such as vascular development and blood pressure regulation [48], erythrocyte homeostasis [49], and the regulation of cell adhesion [50], targeting this mechanosensitive protein could represent a novel therapeutic strategy. In fact, the therapeutic potential of Piezo1 inhibitors, such as GsMTx4, has been extensively studied in various diseases. For instance, targeting Piezo1 with GsMTx4 has been shown to alleviate the severity of osteoarthritis [51]; blocking Piezo1 with GsMTx4 has been demonstrated to reduce the increased pulmonary capillary permeability induced by elevated blood pressure [33]; and GsMTx4 has been reported to improve heart hypertrophy mediated by Piezo1 activation in rats [52]. Recently, the potential of GsMTx4 as a cancer therapy has also begun to be explored. In prostate cancer cells, GsMTx4 inhibits the Akt/mTOR pathway by blocking the Piezo1 channel, thereby exerting anti-cancer effects [13]. In breast cancer, GsMTx4 suppressed cell migration and invasion [53]. However, to date, there has been no research on the therapeutic effects of GsMTx4 in cervical cancer. Current treatment options for advanced or recurrent cervical cancer lack significant breakthroughs in efficacy, and combination therapies may hold potential as a treatment strategy. Targeted inhibition of Piezo1 could serve as a promising approach for combination therapy.

In summary, our study confirmed that Piezo1 was highly expressed in cervical cancer and promoted actin cytoskeleton remodeling in cervical cancer cells through the RhoA/ROCK1/PIP2 pathway, thereby enhancing the invasion and migration of cervical cancer. Piezo1 may serve as a potential therapeutic target for cervical cancer. Future research on the development of novel drugs targeting Piezo1 or combination therapies involving Piezo1 inhibitors could hold significant implications for the treatment of cervical cancer.

**Acknowledgements** The authors would like to express their gratitude to all the faculty members of the Department of Obstetrics and Gynecology at Renmin Hospital of Wuhan University for their technical assistance. This work was supported by the Natural Science Foundation of Hubei Province of China (2021CFB430), the National Natural Science Foundation of China (grant no. 82301828) and the Fundamental Research Funds for the Central Universities (grant no.2042022kf1110).

**Author contributions** All authors contributed to the conception and design of the study. JD, YL, and LZ drafted the manuscript and conducted the experiments. WL and TL were responsible for specimen collection and data processing. FS revised the manuscript. All authors have read and approved the final version of the manuscript for publication.

**Data availability** All data generated or analysed during this study are included in this published article and its supplementary information files.

## Declarations

**Ethics approval and consent to participate** All participants provided informed consent and the study was reviewed and approved by the Ethics Committee of Renmin Hospital of Wuhan University (ethics number: WDRY2023-K092). All the experiments in this study were conducted in compliance with the Declaration of Helsinki.

**Competing interests** The authors declare no competing interests.



## References

1. Bray F, et al. Global cancer statistics 2018: GLOBOCAN estimates of incidence and mortality worldwide for 36 cancers in 185 countries. CA Cancer J Clin. 2018;68:394–424.
2. Sung H, et al. Global cancer statistics 2020: GLOBOCAN estimates of incidence and mortality worldwide for 36 cancers in 185 countries. CA Cancer J Clin. 2021;71:209–49.
3. Guan X. Cancer metastases: challenges and opportunities. Acta Pharm Sin B. 2015;5:402–18.
4. Mauricio D, Zeybek B, Tymon-Rosario J, Harold J, Santin AD. Immunotherapy in cervical cancer. Curr Oncol Rep. 2021;23:61.
5. Yang L, et al. Pin1/YAP pathway mediates matrix stiffness-induced epithelial-mesenchymal transition driving cervical cancer metastasis via a non-Hippo mechanism. Bioeng Transl Med. 2023;8: e10375.
6. Polyak K, Weinberg RA. Transitions between epithelial and mesenchymal states: acquisition of malignant and stem cell traits. Nat Rev Cancer. 2009;9:265–73.
7. Kalluri R, Neilson EG. Epithelial-mesenchymal transition and its implications for fibrosis. J Clin Invest. 2003;112:1776–84.
8. Yilmaz M, Christofori G. EMT, the cytoskeleton, and cancer cell invasion. Cancer Metastasis Rev. 2009;28:15–33.
9. Peng JM, et al. Actin cytoskeleton remodeling drives epithelial-mesenchymal transition for hepatoma invasion and metastasis in mice. Hepatology. 2018;67:2226–43.
10. Miyamoto T, et al. Functional role for Piezo1 in stretch-evoked Ca(2)(+) influx and ATP release in urothelial cell cultures. J Biol Chem. 2014;289:16565–75.
11. Yang XN, et al. Piezo1 is as a novel trefoil factor family 1 binding protein that promotes gastric cancer cell mobility in vitro. Dig Dis Sci. 2014;59:1428–35.
12. Li C, et al. Piezo1 forms mechanosensitive ion channels in the human MCF-7 breast cancer cell line. Sci Rep. 2015;5:8364.
13. Han Y, et al. Mechanosensitive ion channel Piezo1 promotes prostate cancer development through the activation of the Akt/mTOR pathway and acceleration of cell cycle. Int J Oncol. 2019;55:629–44.
14. Gottlieb PA, Bae C, Sachs F. Gating the mechanical channel Piezo1: a comparison between whole-cell and patch recording. Channels (Austin). 2012;6:282–9.
15. Zhang J, et al. PIEZO1 functions as a potential oncogene by promoting cell proliferation and migration in gastric carcinogenesis. Mol Carcinog. 2018;57:1144–55.
16. Liao W, et al. The activation of Piezo1 channel promotes invasion and migration via the release of extracellular ATP in cervical cancer. Pathol Res Pract. 2024;260: 155426.
17. Janmey PA, Bucki R, Radhakrishnan R. Regulation of actin assembly by PI(4,5)P2 and other inositol phospholipids: an update on possible mechanisms. Biochem Biophys Res Commun. 2018;506:307–14.
18. Yin HL, Janmey PA. Phosphoinositide regulation of the actin cytoskeleton. Annu Rev Physiol. 2003;65:761–89.
19. Honigmann A, et al. Phosphatidylinositol 4,5-bisphosphate clusters act as molecular beacons for vesicle recruitment. Nat Struct Mol Biol. 2013;20:679–86.

20. Huang CL. Complex roles of PIP2 in the regulation of ion channels and transporters. Am J Physiol Renal Physiol. 2007;293:F1761–5.
21. Zhang H, et al. LRRC8A as a central mediator promotes colon cancer metastasis by regulating PIP5K1B/PIP2 pathway. Biochim Biophys Acta Mol Basis Dis. 2024;1870: 167066.
22. Sun Y, Thapa N, Hedman AC, Anderson RA. Phosphatidylinositol 4,5-bisphosphate: targeted production and signaling. BioEssays. 2013;35:513–22.
23. Chong J, et al. Modeling of full-length Piezo1 suggests importance of the proximal N-terminus for dome structure. Biophys J. 2021;120:1343–56.
24. Li J, Russell B. Phosphatidylinositol 4,5-bisphosphate regulates CapZbeta1 and actin dynamics in response to mechanical strain. Am J Physiol Heart Circ Physiol. 2013;305:H1614–23.
25. Huang D, et al. Hypoxia induces actin cytoskeleton remodeling by regulating the binding of CAPZA1 to F-actin via PIP2 to drive EMT in hepatocellular carcinoma. Cancer Lett. 2019;448:117–27.
26. Nagai T, Mizuno K. Jasplakinolide induces primary cilium formation through cell rounding and YAP inactivation. PLoS One. 2017;12: e0183030.
27. Oliveira CA, Chedraoui S, Mantovani B. Latrunculin A is a potent inducer of aggregation of polymorphonuclear leukocytes. Life Sci. 1997;61:603–9.
28. Bedell SL, Goldstein LS, Goldstein AR, Goldstein AT. Cervical cancer screening: past, present, and future. Sex Med Rev. 2020;8:28–37.
29. Feng CH, Mell LK, Sharabi AB, McHale M, Mayadev JS. Immunotherapy with radiotherapy and chemoradiotherapy for cervical cancer. Semin Radiat Oncol. 2020;30:273–80.
30. Fife CM, McCarroll JA, Kavallaris M. Movers and shakers: cell cytoskeleton in cancer metastasis. Br J Pharmacol. 2014;171:5507–23.
31. Mitchell MJ, et al. Lamin A/C deficiency reduces circulating tumor cell resistance to fluid shear stress. Am J Physiol Cell Physiol. 2015;309:C736–46.
32. Gudipaty SA, et al. Mechanical stretch triggers rapid epithelial cell division through Piezo1. Nature. 2017;543:118–21.
33. Friedrich EE, et al. Endothelial cell Piezo1 mediates pressure-induced lung vascular hyperpermeability via disruption of adherens junctions. Proc Natl Acad Sci U S A. 2019;116:12980–5.
34. Revathidevi S, Murugan AK, Nakaoka H, Inoue I, Munirajan AK. APOBEC: a molecular driver in cervical cancer pathogenesis. Cancer Lett. 2021;496:104–16.
35. Moujaber O, Stochaj U. The cytoskeleton as regulator of cell signaling pathways. Trends Biochem Sci. 2020;45:96–107.
36. Wen Q, Janmey PA. Polymer physics of the cytoskeleton. Curr Opin Solid State Mater Sci. 2011;15:177–82.
37. Jacinto E, et al. Mammalian TOR complex 2 controls the actin cytoskeleton and is rapamycin insensitive. Nat Cell Biol. 2004;6:1122–8.
38. Geng J, et al. TLR4 signalling via Piezo1 engages and enhances the macrophage mediated host response during bacterial infection. Nat Commun. 2021;12:3519.
39. Liu J, Yang Y, Liu Y. Piezo1 plays a role in optic nerve head astrocyte reactivity. Exp Eye Res. 2021;204: 108445.
40. Li YM, et al. Piezo1 promoted hepatocellular carcinoma progression and EMT through activating TGF-beta signaling by recruiting Rab5c. Cancer Cell Int. 2022;22:162.
41. Thapa N, Anderson RA. PIP2 signaling, an integrator of cell polarity and vesicle trafficking in directionally migrating cells. Cell Adh Migr. 2012;6:409–12.
42. Yamamoto M, et al. Phosphatidylinositol 4,5-bisphosphate induces actin stress-fiber formation and inhibits membrane ruffling in CV1 cells. J Cell Biol. 2001;152:867–76.
43. Borbiro I, Badheka D, Rohacs T. Activation of TRPV1 channels inhibits mechanosensitive Piezo channel activity by depleting membrane phosphoinositides. Sci Signal. 2015;8:ra15.
44. Wei L, Surma M, Shi S, Lambert-Cheatham N, Shi J. Novel insights into the roles of rho kinase in cancer. Arch Immunol Ther Exp (Warsz). 2016;64:259–78.
45. Li X, et al. Calcium and TRPV4 promote metastasis by regulating cytoskeleton through the RhoA/ROCK1 pathway in endometrial cancer. Cell Death Dis. 2020;11:1009.
46. Qi Y, et al. RhoA/ROCK pathway activation is regulated by AT1 receptor and participates in smooth muscle migration and dedifferentiation via promoting actin cytoskeleton polymerization. Int J Mol Sci. 2020. https://doi.org/10.3390/ijms21155398.
47. Xiong Y, et al. Piezo1 activation facilitates ovarian cancer metastasis via Hippo/YAP signaling axis. Channels (Austin). 2022;16:159–66.
48. Li J, et al. Piezo1 integration of vascular architecture with physiological force. Nature. 2014;515:279–82.
49. Cahalan SM, et al. Piezo1 links mechanical forces to red blood cell volume. elife. 2015. https://doi.org/10.7554/eLife.07370.
50. McHugh BJ, et al. Integrin activation by Fam38A uses a novel mechanism of R-Ras targeting to the endoplasmic reticulum. J Cell Sci. 2010;123:51–61.
51. Wang S, et al. Mechanical overloading induces GPX4-regulated chondrocyte ferroptosis in osteoarthritis via Piezo1 channel facilitated calcium influx. J Adv Res. 2022;41:63–75.
52. Zhang Y, et al. Piezo1-mediated mechanotransduction promotes cardiac hypertrophy by impairing calcium homeostasis to activate calpain/calcineurin signaling. Hypertension. 2021;78:647–60.
53. Luo M, et al. Compression enhances invasive phenotype and matrix degradation of breast cancer cells via Piezo1 activation. BMC Mol Cell Biol. 2022;23:1.